Topological Control of Synchronization Patterns: Trading Symmetry for Stability

Joseph D. Hart, Yuanzhao Zhang, Rajarshi Roy, and Adilson E. Motter

Phys. Rev. Lett. **122**, 058301 — Published 8 February 2019

DOI: 10.1103/PhysRevLett.122.058301

Topological Control of Synchronization Patterns: Trading Symmetry for Stability

Joseph D. Hart,[1,2] Yuanzhao Zhang,[3] Rajarshi Roy,[1,2,4] and Adilson E. Motter[3,5]

[1] *Institute for Research in Electronics and Applied Physics, University of Maryland, College Park, Maryland 20742, USA*
[2] *Department of Physics, University of Maryland, College Park, Maryland 20742, USA*
[3] *Department of Physics and Astronomy, Northwestern University, Evanston, Illinois 60208, USA*
[4] *Institute for Physical Science and Technology, University of Maryland, College Park, Maryland 20742, USA*
[5] *Northwestern Institute on Complex Systems, Northwestern University, Evanston, Illinois 60208, USA*

Symmetries are ubiquitous in network systems and have profound impacts on the observable dynamics. At the most fundamental level, many synchronization patterns are induced by underlying network symmetry, and a high degree of symmetry is believed to enhance the stability of identical synchronization. Yet, here we show that the synchronizability of almost any symmetry cluster in a network of identical nodes can be enhanced precisely by breaking its structural symmetry. This counterintuitive effect holds for generic node dynamics and arbitrary network structure and is, moreover, robust against noise and imperfections typical of real systems, which we demonstrate by implementing a state-of-the-art optoelectronic experiment. These results lead to new possibilities for the topological control of synchronization patterns, which we substantiate by presenting an algorithm that optimizes the structure of individual clusters under various constraints.

Symmetry and synchronization are interrelated concepts in network systems. Synchronization, being a symmetric state among oscillators, has its existence and stability influenced by the symmetry of the network [1–3]. For example, recent research has shown that network symmetry can be systematically explored to identify stable synchronization patterns in complex networks [4]. Different work has shown that structural homogeneity (and hence a higher degree of network symmetry) usually enhances synchronization stability [5–7]. Any given network of identical oscillators can always be partitioned into so-called symmetry clusters [8], characterized as clusters of oscillators that are identically coupled, both within the cluster and to the rest of the network, making them natural candidates for cluster synchronization [4, 9]. Cluster synchronization has been investigated in numerous experimental systems, including networks of optoelectronic oscillators [4, 9, 10], semiconductor lasers [11, 12], Boolean systems [13], neurons [14], slime molds [15], and chemical oscillators [16]. Many of these experiments explicitly investigated the beneficial impact of network symmetries on cluster formation [4, 9, 15–17]. Taken together, previous results support the expectation that oscillators that are indistinguishable on structural grounds are also more likely to exhibit indistinguishable (synchronous) dynamics.

In this Letter, we investigate the relation between symmetry and synchronization in the general context of cluster synchronization. We show that, in order to induce stable synchronization, one often has to break the underlying structural symmetry. This counterintuitive result holds for the general class of networks of diffusively coupled identical oscillators with a bounded and connected stability region, and follows rigorously from our demonstration that almost all clusters exhibiting optimal synchronizability are necessarily asymmetric. In particular, the synchronizability of almost any symmetry cluster can be enhanced precisely by breaking the internal structural symmetry of the cluster. These findings add an important new dimension to the recent discovery of *parametric* asymmetry-induced synchronization [18–20], a scenario in which the synchronization of identically coupled identical oscillators is enhanced by setting non-identical parameters to the oscillators. Here, we show that synchronization of identically coupled identical oscillators is enhanced by changing the connection patterns of the oscillators to be non-identical. We refer to this effect as *structural* asymmetry-induced synchronization (AISync). We confirm that this behavior is robust against noise and can be found in real systems by providing the first experimental demonstration of structural AISync using networks of coupled optoelectronic oscillators. In excellent agreement with theory, the experiments show unequivocally that both intertwined and non-intertwined clusters can be optimized by reducing structural symmetry.

We consider a network of n diffusively coupled identical oscillators,

$$\dot{\boldsymbol{x}}_i = \boldsymbol{f}(\boldsymbol{x}_i) - \sigma \sum_{j=1}^{n} L_{ij} \boldsymbol{h}(\boldsymbol{x}_j), \tag{1}$$

where $\boldsymbol{x}_i$ is the state of the i-th oscillator, $\boldsymbol{f}$ is the vector field governing the uncoupled dynamics of each oscillator, $\boldsymbol{L} = \{L_{ij}\}$ is the Laplacian matrix describing the structure of an arbitrary unweighed network, $\boldsymbol{h}$ is the interaction function, and $\sigma > 0$ is the coupling strength. We are interested in the dynamics inside a symmetry cluster. To facilitate presentation, we first assume that the cluster is non-intertwined [4, 21]; that is, it can synchronize independent of whether other clusters synchronize or not. The general case of intertwined clusters—in which desynchronization in one cluster can lead to loss of synchrony in another cluster—requires considering the intertwined clusters concurrently, and this important case is addressed below.

Numbering the oscillators in that cluster from 1 to m, we obtain the dynamical equation for the cluster:

$$\begin{aligned}\dot{\boldsymbol{x}}_i &= \boldsymbol{f}(\boldsymbol{x}_i) - \sigma \sum_{j=1}^{m} L_{ij}\boldsymbol{h}(\boldsymbol{x}_j) + \sigma \sum_{j=m+1}^{n} A_{ij}\boldsymbol{h}(\boldsymbol{x}_j) \\ &= \boldsymbol{f}(\boldsymbol{x}_i) - \sigma \sum_{j=1}^{m} L_{ij}\boldsymbol{h}(\boldsymbol{x}_j) + \sigma \boldsymbol{I}\big(\{\boldsymbol{x}_j\}_{j>m}\big),\end{aligned} \tag{2}$$

where $L_{ij} = \delta_{ij}\mu_i - A_{ij}$, $\boldsymbol{A} = \{A_{ij}\}$ is the adjacency matrix of the network, μ_i is the indegree of node i, and the equation holds for $1 \le i \le m$. Here, we denote the input term from the rest of the network $\sum_{j=m+1}^{n} A_{ij}\boldsymbol{h}(\boldsymbol{x}_j)$ by $\boldsymbol{I}\big(\{\boldsymbol{x}_j\}_{j>m}\big)$ to emphasize that this term is independent of i and hence equal for all oscillators $1,\dots,m$. This term is zero, and $m = n$, only in the special case in which the entire network consists of a single symmetry cluster.

For $m < n$, if we regard the cluster subnetwork consisting of oscillators $1,\dots,m$ as a separate network (by ignoring its connections with other clusters), then the corresponding $m \times m$ Laplacian matrix $\widetilde{\boldsymbol{L}}$ is closely related to the corresponding block of the $n \times n$ Laplacian matrix $\boldsymbol{L}$ of the full network:

$$L_{ij} = \begin{cases} \widetilde{L}_{ij}, & 1 \le i \ne j \le m, \\ \widetilde{L}_{ij} + \widetilde{\mu}, & 1 \le i = j \le m, \end{cases} \tag{3}$$

where $\widetilde{\mu} > 0$ is the number of connections each oscillator in the cluster receives from the rest of the network. It is then clear that there are two differences in the dynamical equation when the cluster subnetwork is part of a larger network (i.e., as a symmetry cluster, described by Eq. (2)) rather than as an isolated network. First, the Laplacian matrix $\widetilde{\boldsymbol{L}}$ in the dynamical equation is replaced by $\widehat{\boldsymbol{L}} = \{L_{ij}\}_{1\le i,j\le m} = \widetilde{\boldsymbol{L}} + \widetilde{\mu}\mathbb{1}_m$; that is, the diagonal entries are uniformly increased by $\widetilde{\mu}$. Second, each oscillator now receives a common input $\sigma\boldsymbol{I}\big(\{x_j\}_{j>m}\big)$ produced by its coupling with other clusters, which generally alters the synchronization trajectory $\boldsymbol{s}_I \equiv \boldsymbol{x}_1 = \cdots = \boldsymbol{x}_m$, causing it to be typically different from the ones generated by the uncoupled dynamics $\dot{\boldsymbol{s}} = \boldsymbol{f}(\boldsymbol{s})$. This has to be accounted for in calculating the maximum Lyapunov exponent transverse to the cluster synchronization manifold to determine the stability of the cluster synchronous state.

Despite these differences, a diagonalization procedure similar to the one used in the master stability function approach [22] can still be applied to the variational equation in order to assess the cluster's synchronization stability. The variational equation describing the evolution of the deviation away from $\boldsymbol{s}_I$ inside the cluster can be written as

$$\delta\dot{\boldsymbol{X}} = \Big(\mathbb{1}_m \otimes J\boldsymbol{f}(\boldsymbol{s}_I) - \sigma\widehat{\boldsymbol{L}} \otimes J\boldsymbol{h}(\boldsymbol{s}_I)\Big)\,\delta\boldsymbol{X}, \tag{4}$$

where $\delta\boldsymbol{X} = (\delta\boldsymbol{x}_1^\intercal,\cdots,\delta\boldsymbol{x}_m^\intercal)^\intercal = (\boldsymbol{x}_1^\intercal - \boldsymbol{s}_I^\intercal,\cdots,\boldsymbol{x}_m^\intercal - \boldsymbol{s}_I^\intercal)^\intercal$ and $\otimes$ denotes the Kronecker product. The rest of the network does not enter the equation explicitly, other than through its influence on the coupling matrix $\widehat{\boldsymbol{L}}$ and the synchronization trajectory $\boldsymbol{s}_I$. If $\widehat{\boldsymbol{L}}$ is diagonalizable (as for any undirected network), the decoupling of Eq. (4) results in m independent d-dimensional equations corresponding to individual perturbation modes:

$$\dot{\boldsymbol{\eta}}_i = \big[J\boldsymbol{f}(\boldsymbol{s}_I) - \sigma\widehat{v}_i J\boldsymbol{h}(\boldsymbol{s}_I)\big]\boldsymbol{\eta}_i, \tag{5}$$

where d is the dimension of node dynamics, J is the Jacobian operator, $\boldsymbol{\eta} = (\boldsymbol{\eta}_1^\intercal,\cdots,\boldsymbol{\eta}_m^\intercal)^\intercal$ is $\delta\boldsymbol{X}$ expressed in the new coordinates that diagonalize $\widehat{\boldsymbol{L}}$, and $\widehat{v}_i = \widetilde{v}_i + \widetilde{\mu}$ are the eigenvalues of $\widehat{\boldsymbol{L}}$ in ascending order of their real parts [with $\{\widetilde{v}_i\} = \mathrm{eig}(\widetilde{\boldsymbol{L}})$]. If $\widehat{\boldsymbol{L}}$ is not diagonalizable [23], the analysis can be carried out by using the Jordan canonical form of this matrix to replace diagonalization by block-diagonalization, as explicitly shown in the Supplemental Material [24]. In both cases the cluster synchronous state is stable if $\Lambda(\sigma\widehat{v}_i) < 0$ for $i = 2,\dots,m$, where Λ is the largest Lyapunov exponent of Eq. (5) and $\widehat{v}_2,\cdots,\widehat{v}_m$ represent the transverse modes; the maximum transverse Lyapunov exponent (MTLE) determining the stability of the synchronous state is $\max_i \Lambda(\sigma\widehat{v}_i)$. Moreover, for the large class of oscillator networks for which the stability region is bounded and connected [25–28], as assumed here and verified for all models we consider [29], the synchronizability of the symmetry cluster can be quantified in terms of the eigenratio $R = \mathrm{Re}(\widetilde{v}_m)/\mathrm{Re}(\widetilde{v}_2)$: the smaller this ratio, in general the larger the range of σ over which the cluster synchronous state can be stable. The cluster subnetwork is most synchronizable when $\widehat{v}_2 = \cdots = \widehat{v}_m$, which also implies that all eigenvalues are real and in fact integers if the network is unweighted as considered here [30]. It is important to notice that the optimality of the cluster subnetwork and associated properties are conserved in the sense that if $\widetilde{v}_2 = \cdots = \widetilde{v}_m$ for the isolated cluster, then $\widehat{v}_2 = \cdots = \widehat{v}_m$ will hold for the cluster as part of a larger network. Since the analysis above does not invoke the continuity of the equations anywhere, it holds for discrete-time systems as well. In this case one can simply replace $\delta\dot{\boldsymbol{X}}$ and $\delta\boldsymbol{X}$ in Eq. (4) by $\delta\boldsymbol{X}(t+1)$ and $\delta\boldsymbol{X}(t)$, respectively.

Now we can compare symmetry clusters with optimal clusters and show rigorously that almost all optimally synchronizable clusters are asymmetric. Without loss of generality, we consider an unweighted cluster in isolation and assume it has m nodes and ℓ directed links internal to the cluster. In a symmetry cluster, because the nodes are structurally identical, the in- and out-degrees of all nodes must be equal. Thus, ℓ must be divisible by m if the cluster is symmetric. In an optimal cluster, because $\widetilde{v}_2 = \cdots = \widetilde{v}_m \equiv \widetilde{v}$ and thus $\mathrm{tr}(\widetilde{\boldsymbol{L}}) = (m-1)\widetilde{v}$, it follows that $\widetilde{v} = \ell/(m-1)$. The fact that $\widetilde{v}$ is an integer implies that ℓ must be divisible by $m-1$ if the cluster is optimal. Since $\ell \le m(m-1)$, the two divisibility conditions can

symmetry clusters	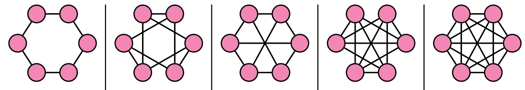				
eigenratio	4	2.5	2	1.5	1
optimal clusters	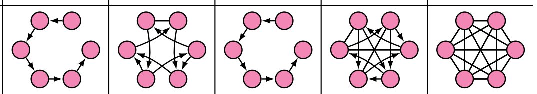				
eigenratio	1	1	1	1	1

TABLE I. Connected symmetry clusters of 6 nodes and optimal clusters embedded within them. Some symmetry clusters have more than one embedded optimal network, in which case we show one that can be obtained through a minimal number of link deletions.

be satisfied simultaneously if and only if $\ell = m(m-1)$ (i.e., when the network is a complete graph). But there are numerous optimal networks (and hence clusters) for $\ell < m(m-1)$ [23, 30]. Therefore, for any given number m of nodes, all optimal clusters other than the complete graph are necessarily asymmetric, meaning that (with the exception of the complete graph) the synchronization stability of any symmetry cluster can be improved by breaking its structural symmetry. This general conclusion forms the basis of structural AISync and holds, in particular, when an entire network consists of a single symmetry cluster (as illustrated below).

When viewed as isolated subnetworks, symmetry clusters are equivalent to the vertex-transitive digraphs in algebraic graph theory, defined as directed graphs in which every pair of nodes is equivalent under some node permutation [31, 32]. Thus, in order to improve the stability of any non-intertwined symmetry cluster from an arbitrary network, we only need to optimize the corresponding vertex-transitive digraph by manipulating its (internal) links. In particular, this can always be done by removing links inside the symmetry cluster [30, 33], despite the fact that sparser networks are usually harder to synchronize. For concreteness, we focus on clusters that are initially undirected and consider the selective removal of individual directional links. As an example, we show in Table I all connected undirected symmetry clusters of 6 nodes and their embedded optimal networks. Apart from the complete graph, which is already optimal to begin with, the synchronizability of the other symmetry clusters as measured by the eigenratio R is significantly improved in all cases.

Because in practice it can be costly or unnecessary to fully optimize a symmetry cluster, it is natural to ask whether its synchronizability can be significantly improved by just modifying a few links. We developed an efficient algorithm for this purpose and summarize the statistical results based on all connected undirected symmetry clusters of sizes between $m = 8$ and 17 in the Supplemental Material [24]. On average, only about 14% of the links need to be rewired to reduce $R - 1$ by half and thus significantly improve synchronizability of symmetry clusters. This illustrates the potential of structural AISync as a mechanism for the topological control of synchronization stability. Our simulated annealing code to improve cluster synchronizability is available at [34]. This algorithm can also be used to demonstrate structural AISync in global synchronization, as shown in the Supplemental Material [24].

Having established a theoretical foundation for our main finding, we now turn to our experimental results. The experiments are performed using networks of identical optoelectronic oscillators whose nonlinear component is a Mach-Zehnder intensity modulator. The system can be modeled as

$$x_i(t+1) = \beta I[x_i(t)] - \sigma \sum_{j=1}^{n} L_{ij} I[x_j(t)] \mod 2\pi, \quad (6)$$

where t is now a discrete time, β is the feedback strength, $I(x_i) = \sin^2(x_i + \delta)$ is the normalized intensity output of the modulator, x_i is the normalized voltage applied to the modulator, and δ is the operating point (set to $\pi/4$ in our experiments). Each oscillator consists of a clocked optoelectronic feedback loop. Light from a 780 nm continuous-wave laser passes through the modulator, which provides the nonlinearity. The light intensity is converted into an electrical signal by a photoreceiver and measured by a field-programmable gate array (FPGA) via an analog-to-digital converter (ADC). The FPGA is clocked at 10 kHz, resulting in the discrete time map dynamics of the oscillators. The FPGA controls a digital-to-analog converter (DAC) that drives the modulator with a voltage $x_i(t+1) = \beta I[x_i(t)]$, closing the feedback loop. The oscillators are coupled together electronically on the FPGA according to the desired Laplacian matrix. Specifically, the experimental system uses time-multiplexing and time delays to realize a network of coupled oscillators from a single time-delayed feedback loop, as described in detail in Ref. [35]. A schematic illustration of the experimental setup can be found in the Supplemental Material [24].

We first consider the network configuration shown in Fig. 1(a), which is a complex network with five symmetry clusters. The symmetry cluster highlighted in magenta is non-intertwined, and can be optimized by removing the red dashed links. The MTLE calculation in Fig. 1(b) predicts AISync to be common in the parameter space. Fixing $\beta = 6$, we performed 8 runs of the experiment starting from different random initial conditions, and measured the normalized voltages x_i for 8196 iterations at each fixed coupling strength before increasing σ by 0.015. The synchronization error is defined as $\Delta = \sqrt{\sum_{1 \le i \le m} \|x_i - \bar{x}\|^2 / m}$, where $\bar{x}$ is the mean inside the cluster. The data points in Fig. 1(c) correspond to the average synchronization error $\langle \Delta \rangle$, defined as Δ av-

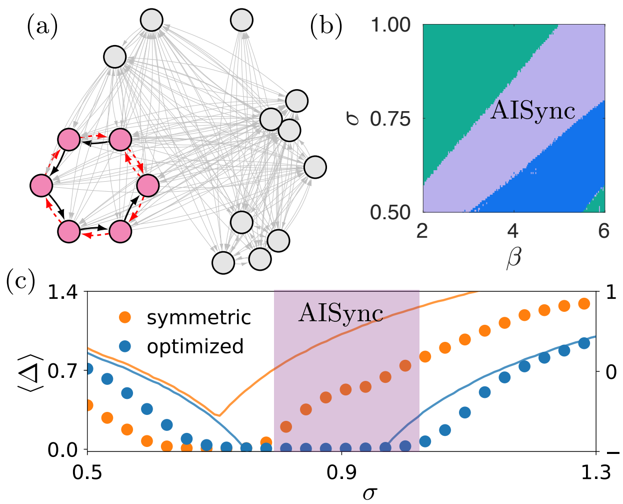

FIG. 1. Experimental demonstration of structural AISync in a non-intertwined cluster. (a) Example network in which a symmetry cluster (magenta) is optimized for synchronization by removing the red links. (b) Predictions based on the theoretical computation of the MTLE, showing that in the $\sigma \times \beta$ parameter space there is an AISync region (purple); the other colors indicate the regions where both clusters synchronize (blue) and where neither cluster can synchronize (green). (c) Experimentally measured average synchronization error $\langle \Delta \rangle$ in the original (orange) and optimized (blue) cluster for $\beta = 6$. The experimental results are in good agreement with the MTLE calculations (color-coded curves).

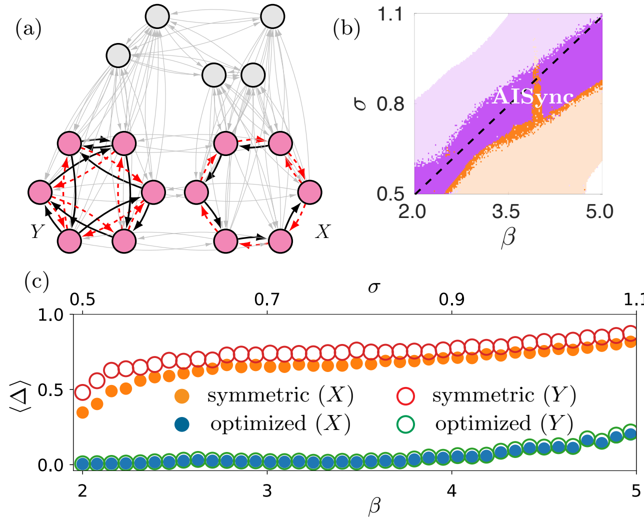

FIG. 2. Demonstration of structural AISync in intertwined clusters. (a) Network in which two intertwined clusters (magenta) are optimized to induce synchronization by removing the red links. (b) Region in the $\sigma \times \beta$ parameter space satisfying the condition in Eq. (7), which is expanded from the orange shaded area to include the purple shaded area when the clusters are optimized. The dark shades (orange and purple) highlight the AISync region determined through direct simulations. (c) Experimentally measured average synchronization error $\langle \Delta \rangle$ in the original and optimized clusters when moving through the parameter space quasi-statically along the dashed line in (b).

eraged over the last 5000 iterations for each σ and then further averaged over the 8 experimental runs. The error bars corresponding to the standard deviation across different runs are smaller than the size of the symbols. One can observe AISync over a wide range of the coupling strength σ, matching the theoretical prediction. Structural AISync is also common for different oscillator types and network structures and is robust against noise and parameter mismatches, as demonstrated systematically in the Supplemental Material [24].

We now turn to the case of intertwined clusters. Consider two intertwined clusters X and Y subject to transverse perturbations $\delta\boldsymbol{X}$ and $\delta\boldsymbol{Y}$, respectively. The variational equation for $\delta\boldsymbol{X}$ has the same form as Eq. (4) except for an additional cross-coupling term $\sigma\boldsymbol{C} \otimes J\boldsymbol{h}(\boldsymbol{s}_{I_Y})\delta\boldsymbol{Y}$ added to the right, where $\boldsymbol{C}$ is the adjacency matrix describing the inter-cluster coupling from cluster Y to cluster X. The variational equation for $\delta\boldsymbol{Y}$ is defined similarly. Now, if $\delta\boldsymbol{X}$ ($\delta\boldsymbol{Y}$) does not converge to zero according to Eq. (4), then the cross-coupling term must not vanish and $\|\delta\boldsymbol{Y}\|$ ($\|\delta\boldsymbol{X}\|$) must stay away from zero in order for $\|\delta\boldsymbol{X}\| \to 0$ ($\|\delta\boldsymbol{Y}\| \to 0$) in the complete variational equation. Thus, in order to stabilize synchronization in intertwined clusters, the following condition must be satisfied for each cluster:

$$\|\boldsymbol{\eta}_i\| \to 0 \text{ in Eq. (5) for all transverse modes.} \qquad (7)$$

In other words, $\|\delta\boldsymbol{X}\|$ and $\|\delta\boldsymbol{Y}\|$ converging to zero in Eq. (4) is a necessary condition for stable synchronization in X and Y. Because optimizing the clusters independently (as if they were non-intertwined) is guaranteed to expand the region satisfying the condition in Eq. (7), such independent optimization is an effective strategy for improving synchronization in intertwined clusters. For more details on this analysis, see Supplemental Material [24].

We demonstrate the strength of our approach on a random network containing two intertwined clusters, which are highlighted in Fig. 2(a). Each cluster is optimized by removing the red dashed links, which breaks the structural symmetry but reduces the eigenratio of the cluster to 1. The orange shade in Fig. 2(b) indicates the region where the condition in Eq. (7) is satisfied by the original clusters. The region satisfying this condition is expanded to include the purple region when the clusters are optimized. Direct simulations allow us to identify a large parameter region exhibiting AISync, which is highlighted in dark shades in Fig. 2(b) and is included mainly in the expanded (purple) region. A small portion of the AISync region also extends into the orange region, which follows from the condition in Eq. (7) being necessary but not sufficient for synchronization in the original clusters. To validate the theory and the numerics, we perform experiments with parameters varied quasi-statically along the dashed line in Fig. 2(b). As shown in Fig. 2(c), the symmetry clusters are both incoherent for the entire range of parameters studied. The two optimized clusters exhibit perfectly synchronized dynamics except at the very edge of the AISync region, where the noise in the ADC has a marked impact on the dynamics (nevertheless, they are still much more synchronized than the symmetry clusters).

In summary, we established the role of structural asymmetry (or structural heterogeneity) in promoting spontaneous synchronization through both theory and experiments. Our theory confirmed the generality of the phenomenon, while our experiments demonstrated its robustness. Because symmetry clusters arise naturally in complex networks, our findings are applicable to a wide range of coupled dynamical systems. In particular, since identical synchronization in a symmetry cluster is the basic building block of more complex synchronization patterns, our results can be used for the *targeted* topological control of cluster synchronization in complex networks, which echoes the positive effect of structural asymmetry on input control [36].

The authors thank Alex Mercanti, Takashi Nishikawa, Don Schmadel, and Thomas E. Murphy for insightful discussions. This work was supported by ONR Grant No. N000141612481 (JDH and RR) and ARO Grant No. W911NF-15-1-0272 (YZ and AEM). JDH and YZ contributed equally to this work.

[1] I. Stewart, M. Golubitsky, and M. Pivato, Symmetry groupoids and patterns of synchrony in coupled cell networks, SIAM J. Appl. Dyn. Syst. **2**, 609 (2003).

[2] V. Nicosia, M. Valencia, M. Chavez, A. Díaz-Guilera, and V. Latora, Remote synchronization reveals network symmetries and functional modules, Phys. Rev. Lett. **110**, 174102 (2013).

[3] M. Aguiar, P. Ashwin, A. Dias, and M. Field, Dynamics of coupled cell networks: synchrony, heteroclinic cycles and inflation, J. Nonlinear Sci. **21**, 271 (2011).

[4] L. M. Pecora, F. Sorrentino, A. M. Hagerstrom, T. E. Murphy, and R. Roy, Cluster synchronization and isolated desynchronization in complex networks with symmetries, Nat. Commun. **5**, 5079 (2014).

[5] L. Donetti, P. I. Hurtado, and M. A. Munoz, Entangled networks, synchronization, and optimal network topology, Phys. Rev. Lett. **95**, 188701 (2005).

[6] M. Denker, M. Timme, M. Diesmann, F. Wolf, and T. Geisel, Breaking synchrony by heterogeneity in complex networks, Physical review letters **92**, 074103 (2004).

[7] T. Nishikawa, A. E. Motter, Y.-C. Lai, and F. C. Hoppensteadt, Heterogeneity in oscillator networks: Are smaller worlds easier to synchronize?, Phys. Rev. Lett. **91**, 014101 (2003).

[8] B. D. MacArthur, R. J. Sánchez-García, and J. W. Anderson, Symmetry in complex networks, Discrete Appl. Math. **156**, 3525 (2008).

[9] F. Sorrentino, L. M. Pecora, A. M. Hagerstrom, T. E. Murphy, and R. Roy, Complete characterization of the stability of cluster synchronization in complex dynamical networks, Sci. Adv. **2**, e1501737 (2016).

[10] C. R. Williams, T. E. Murphy, R. Roy, F. Sorrentino, T. Dahms, and E. Schöll, Experimental observations of group synchrony in a system of chaotic optoelectronic oscillators, Phys. Rev. Lett. **110**, 064104 (2013).

[11] M. Nixon, M. Fridman, E. Ronen, A. A. Friesem, N. Davidson, and I. Kanter, Controlling synchronization in large laser networks, Phys. Rev. Lett. **108**, 214101 (2012).

[12] A. Argyris, M. Bourmpos, and D. Syvridis, Experimental synchrony of semiconductor lasers in coupled networks, Opt. Express **24**, 5600 (2016).

[13] D. P. Rosin, D. Rontani, D. J. Gauthier, and E. Schöll, Control of synchronization patterns in neural-like Boolean networks, Phys. Rev. Lett. **110**, 104102 (2013).

[14] R. Vardi, R. Timor, S. Marom, M. Abeles, and I. Kanter, Synchronization with mismatched synaptic delays: a unique role of elastic neuronal latency, EPL **100**, 48003 (2012).

[15] A. Takamatsu, R. Tanaka, H. Yamada, T. Nakagaki, T. Fujii, and I. Endo, Spatiotemporal symmetry in rings of coupled biological oscillators of Physarum plasmodial slime mold, Phys. Rev. Lett. **87**, 078102 (2001).

[16] J. F. Totz, R. Snari, D. Yengi, M. R. Tinsley, H. Engel, and K. Showalter, Phase-lag synchronization in networks of coupled chemical oscillators, Phys. Rev. E **92**, 022819 (2015).

[17] J. D. Hart, K. Bansal, T. E. Murphy, and R. Roy, Experimental observation of chimera and cluster states in a minimal globally coupled network, Chaos **26**, 094801 (2016).

[18] T. Nishikawa and A. E. Motter, Symmetric States Requiring System Asymmetry, Phys. Rev. Lett. **117**, 114101 (2016).

[19] Y. Zhang, T. Nishikawa, and A. E. Motter, Asymmetry-induced synchronization in oscillator networks, Phys. Rev. E **95**, 062215 (2017).

[20] Y. Zhang and A. E. Motter, Identical Synchronization of Nonidentical Oscillators: When Only Birds of Different Feathers Flock Together, Nonlinearity **30** (2017).

[21] Y. S. Cho, T. Nishikawa, and A. E. Motter, Stable Chimeras and Independently Synchronizable Clusters, Phys. Rev. Lett. **119**, 084101 (2017).

[22] L. M. Pecora and T. L. Carroll, Master stability functions for synchronized coupled systems, Phys. Rev. Lett. **80**, 2109 (1998).

[23] T. Nishikawa and A. E. Motter, Maximum performance at minimum cost in network synchronization, Physica D **224**, 77 (2006).

[24] Supplemental Material available at [URL].

[25] M. Barahona and L. M. Pecora, Synchronization in small-world systems, Phys. Rev. Lett. **89**, 054101 (2002).

[26] Z. Li, Z. Duan, G. Chen, and L. Huang, Consensus of multiagent systems and synchronization of complex networks: a unified viewpoint, IEEE Trans. Circuits Syst. I, Reg. Papers **57**, 213 (2010).

[27] V. Flunkert, S. Yanchuk, T. Dahms, and E. Schöll, Synchronizing distant nodes: a universal classification of net-

works, Phys. Rev. Lett. **105**, 254101 (2010).

[28] L. Huang, Q. Chen, Y.-C. Lai, and L. M. Pecora, Generic behavior of master-stability functions in coupled nonlinear dynamical systems, Phys. Rev. E **80**, 036204 (2009).

[29] For nonlinear oscillators, this can be done numerically by calculating the master stability function for a sufficiently large region in the complex plane that encompasses all eigenvalues of the coupling matrix scaled by the permissible coupling strength.

[30] T. Nishikawa and A. E. Motter, Network synchronization landscape reveals compensatory structures, quantization, and the positive effect of negative interactions, Proc. Natl. Acad. Sci. U.S.A. **107**, 10342 (2010).

[31] N. Biggs, *Algebraic Graph Theory* (Cambridge University Press, 1993).

[32] B. D. McKay and A. Piperno, Practical graph isomorphism, II, J. Symb. Comput. **60**, 94 (2014).

[33] T. Nishikawa and A. E. Motter, Synchronization is optimal in nondiagonalizable networks, Phys. Rev. E **73**, 065106 (2006).

[34] Simulated annealing code to improve synchronizability through minimal link rewiring, removal, or addition: `https://github.com/y-z-zhang/optimize_sym_cluster/`.

[35] J. D. Hart, D. C. Schmadel, T. E. Murphy, and R. Roy, Experiments with arbitrary networks in time-multiplexed delay systems, Chaos **27**, 121103 (2017).

[36] A. J. Whalen, S. N. Brennan, T. D. Sauer, and S. J. Schiff, Observability and controllability of nonlinear networks: The role of symmetry, Phys. Rev. X **5**, 011005 (2015).

[37] C. Godsil, Eigenvalues of graphs and digraphs, Linear Algebra Appl. **46**, 43 (1982).